A Model Predictive Control Volt/VAr Management System for the Froan network

Johannes P. Maree†
SINTEF Digital Research*

Salman Zaferanlouei
IEL, NTNU*

***Abstract*—This work presents a Volt/VAr Management System, based on a Model Predictive Control strategy, which can be applied for managing dynamic network resilience. Dynamic network resilience, in this context, is associated with resilient microgrid operation (stable voltage profiles within admissible range) during the transition from grid-tied to island-mode operation. In addition, the predictive nature of the framework allows the systematic incorporation of forecasts on intermittent distributed renewable generation capacity and load demands which in turn can be utilized in a optimization based framework to optimally exploit network flexibility. The developed framework is validated for a migrogrid in the municipality of Frøya, Norway.**

I. Introduction

In a relentless drive against time to reduce the disruptive consequences of increased climate change, an international effort is required to curb carbon emissions and reach the ambitious goals stipulated in the Paris Agreement. Two prominent components, identified by the World Energy Transitions Outlook to abate carbon emissions, are renewables in combination with energy conservation and efficiency [1]. The introduction of renewables in the energy mix has however led to numerous challenges in the grid, which among other, power quality is the most prominent concern in relation to end consumers [2]. In the latter, we are concerned with uninterrupted power supply with stable voltage and frequency conditions. Microgrids have been identified as a viable solution to facilitate the integration of renewables in the grid whilst promoting system reliability at the distribution level [3]. In addition, microgrids promote the overall resiliency of power systems with the ability to operate in island-mode during major disturbance events [4].

Hierarchical control has been adopted as a uniform framework for control by The European Network of Transmission System Operators for Electricity (ENTSO-E) [5] which, in principle, differentiates between primary, secondary and tertiary control layers. At the primary level, droop control is often adopted for stabilizing system frequency and voltage with fast response dynamics during power sharing stabilization. Secondary control, which can either be centralized or decentralized, provides steady-state tracking set-points for primary controllers to promote admissible voltage and frequency steady-state recovery and balanced energy flow. Scheduling and planning of dispatchable generation and storage capacity is often associated with the tertiary layer [5]. To address control challenges associated with conventional control methods (mostly cascaded linear control), which fail to satisfactorily handle the complexities and uncertainties associated with the penetration of renewables; Model Predictive Control (MPC) is emerging as a favourable alternative for microgrid applications at pilot stage [6]. (i) Incorporating system constraints in a systematic manner; (ii) taking into account cross-coupling dynamics of complex underlying processes; (iii) implicitly optimizing multiple (often conflicting) operational objectives while taking expected forecasted generation capacity and load demands into account, are just some of the advantages advocated for MPC. MPC strategies for microgrid control can be differentiated between converter-level, and grid-level MPC strategies [6].

In this work, we are primarily concerned with the secondary control layer in which we adopt a grid-level MPC based strategy. This strategy, in principle, entails optimizing system-level operational objectives which, among other, may include optimal power flow and energy balance corrections; and, the dynamic regulation of voltage profiles to promote resilient operation. This strategy is, in principle, concerned with power quality management and can be classified as a Volt/VAr management (VVM) system [7]. VVM systems regulate distribution system voltage profiles by managing the reactive power flows and can contribute towards energy conservation, efficiency and peak reduction targets as advocated by [1]. [8] proposed and validated a VVM strategy defined by a stochastic mixed-integer non-linear program (MINLP) MPC formulation for the IEEE 33 network case. Inherent complexity may render the later strategy computationally intractable for real-time execution on larger networks. [9] addresses computational complexities by considering a distributed VVM strategy by segregating the microgrid into local areas of clustered distributed generation capacity. [10] solves the multi-stage ACOPF problem using a an interior point solver. In the latter, sparsity of the underlying optimization problem is exploited, which when combined with analytic derived expressions of higher order derivatives of the Lagrangian function, promotes computational efficiency. In this work, we solve the multi-stage ACOPF problem in a MPC strategy to define a VVM strategy. In contrast to [10], we use Casadi [11] as an automatic differentiation symbolic framework to evaluate higher order

This work is funded by ROME - Resilient and Optimal Micro-Energy-grid (RCN project number 280797). The authors gratefully acknowledge the financial support from the Research Council of Norway (RCN). Tensio AS, and Iver Sperstad and Merkebu Degefa from SINTEF Energy, are acknowledged for their valuable feedback during discussions.†corresponding author: *phillip.maree@sintef.no*; *Trondheim, Norway

This is the author accepted version of an article published in
2021 IEEE PES Innovative Smart Grid Technologies - Asia (ISGT Asia)
https://doi.org/10.1109/ISGTAsia49270.2021.9715691

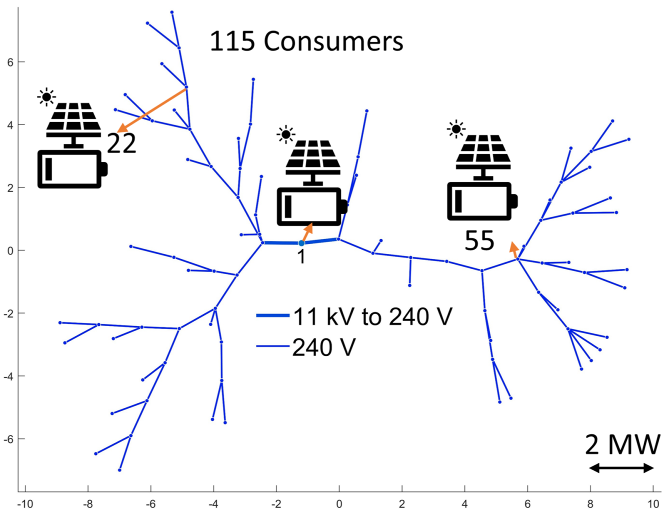

Fig. 1: Local 88-bus distribution grid for the Froan network with bus $i = 1$ being the reference bus. Power transfer distance ($PT_{ij} := \sum_{(i,j)\in\mathcal{N}} |PF_{ij}|$) visualization [13] is adopted defining the cumulative power flow (PF) over all branches $(i, j) \in \mathcal{N}$ with unit power injection at node i and withdrawal from node j.

derivatives, where Ipopt (an interior point based method [12]) is used to efficiently solve a sparse non-linear programming problem (NLP). The multiple stages are temporally linked by considering the temporal dynamics associated with Energy Storage Systems (ESS) and Distributed Generation (DG) units dispatched across the network of interest. The proposed strategy is validated for the Froan network which is based in the municipality of Frøya in Trøndelag county, Norway.

II. Froan network

The Resilient and Optimal Micro-Energy-grid (ROME) project is a joint Indian-Norwegian research project addressing the *smart environments* thematic area with a particular emphasis on the migrogrid for smart grids. Microgrids are considered a pragmatic solution for Norway given the numerous small islands[1] along the west coast of Norway with dilapidated network infrastructure connecting to the main grid. In this context, utilities in particular, need to asses the potential of distribution upgrade deferrals as possible means to ameliorate the high costs associated with replacing weak and old sea cables. The Froan network (see Figure 1), considered as a pilot case study in this work, is classified as a Low-Voltage (LV) network with 115 consumers. The grid was commissioned in 1962, upgraded in 1982, and is connected with the mainland distribution grid via a 23 km sea cable. It is anticipated that this cable needs to be replaced or upgraded soon, however, at the estimated expense of 30 MNOK. Although Froan has no local energy production capacity, it is anticipated that the potential of renewable energy production, in combination with energy storage, may be a viable and cost effective distribution upgrade deferral strategy.

[1]more than 300 islands with a distance larger than 1km from mainland

A. Scenarios

The IEEE PES Industry Technical Support Task Force defines resilience of a network as the inherent ability to withstand and reduce the magnitude and/or the duration of disruptive events. Systems promoting network resilience are, among other, characterized by the ability to anticipate disturbances and has the means to orchestrate sufficient recovery or ride-through mechanisms [14]. A resilient system differentiates itself from a reliable system in the sense that the former is often associated as being robust against low-probability, high-impact events [4]. Scenarios of interest for resilient management, in the context of the Froan network, are: (i) the low-probability, high-impact scenario associated with the Point of Common Contact (PCC) cable failure (unplanned transition from grid-tied to island-mode); and, (ii) utilising network flexibility (enabled by distributed ESS's and emergency diesel DG assets) to absorb the intermittent power generation associated with RES's and load demand uncertainties.

III. Volt/VAr Management System

The VVM System, in principle, defines a MPC strategy that dynamically regulates resilient related metrics[2] over a receding horizon. The ACOPF multiple-segments are linked with each other along the predicted dynamic transients of the respective dispatched ESS's and diesel DG's. The latter, when combined with forecasted scenarios on RES generation and load demands in an all inclusive MPC formulation, allows the definition of a control law that is robust to uncertainty associated with RES's and load demands; while, promoting optimization objective criteria associated with managing resilience during dynamic operation.

A. Optimal power flow and energy balance

For the network branch $(i, j) \in \mathcal{N}$, we consider a Π-branch model with the rectangular coordinates for admittance being $Y^{ij} := G^{ij} + \mathrm{i}B^{ij}$; and, a bus injection model to define the ACOPF at bus $i \in \mathcal{M}$ for time $t = k$ [15]:

$$P^i_k := \sum_{j=1}^{\mathcal{M}} V^i_k V^j_k \left(G^{ij} cos\left(\delta^{ij}_k\right) + B^{ij} sin\left(\delta^{ij}_k\right)\right) \tag{1a}$$

$$Q^i_k := \sum_{j=1}^{\mathcal{M}} V^i_k V^j_k \left(G^{ij} sin\left(\delta^{ij}_k\right) - B^{ij} cos\left(\delta^{ij}_k\right)\right) \tag{1b}$$

We need to satisfy the following energy balance relations for active and reactive power flow

$$P^i_k = P^{G,i}_k - P^{L,i}_k;\; Q^i_k = Q^{G,i}_k - Q^{L,i}_k \tag{2}$$

The energy generation $(P^{G,i}_k, Q^{G,i}_k)$ may, among other, include contributions associated with the import/export of energy via the PCC (here associated with bus $i = 1$); RES (dispatched at nodes $r \in \mathcal{R} \subseteq \mathcal{M}$); ESS (dispatched at $s \in \mathcal{S} \subseteq \mathcal{M}$) and/or DG (dispatched at $d \in \mathcal{D} \subseteq \mathcal{M}$). Load demands $(P^{L,i}_k, Q^{L,i}_k)$ may refer to both critical and controllable load demands (dispatched at $l \in \mathcal{L} \subseteq \mathcal{M}$).

[2]as inferred from observing the dynamic evolution of voltage profiles when solving the multiple-segment ACOPF problem

B. Temporal dynamic association

The static N-stages of (1) are dynamically associated along time $t = k$, $\forall k \in \mathbb{I}_{0:N}$ (via the energy balance relation (2)); applicable to those bus nodes $i \in \mathcal{M}$ who have dispatched ESS and DG assets. The injected power related to ESS, $s \in \mathcal{S}$, are bounded by the maximum ESS storage capacity as modelled by the following discrete Ordinary Dynamic Equations (ODE):

$$SoC_{k+1}^{\mathcal{S},s} = SoC_k^{\mathcal{S},s} + h\left(\eta_c^s P_k^{\mathcal{S}_c,s}/C_{\mathcal{S}}^s - P_k^{\mathcal{S}_d,s}/\eta_d^s C_{\mathcal{S}}^s\right) \quad (3a)$$

$$P_k^{\mathcal{S},s} = P_k^{\mathcal{S}_c,s} - P_k^{\mathcal{S}_d,s};\ 0.1 \leq SoC_k^{\mathcal{S},s} \leq 0.9 \quad (3b)$$

$$(P_k^{\mathcal{S},s})^2 + (Q_k^{\mathcal{S},s})^2 \leq (\mathcal{S}_{max}^s)^2 \quad (3c)$$

in which h, $C_{\mathcal{S}}^s$ and η are the sampling time, ESS capacity (MWh) and charging coefficients, respectively. (3c) is a circular bounded characteristic curve for the inverter of the ESS [16]. Here, $P_k^{\mathcal{S}_c,s} \geq 0; P_k^{\mathcal{S}_d,s} \geq 0$ to prevent simultaneous charge and discharge. Dispatched diesel DG assets, $d \in \mathcal{D}$, may have transient response times being substantially lower than that associated with typical ESS assets (i.e., switching of ultra capacitor banks). To such an extent, to model slow transient behaviour of DG assets, and their energy contributions towards (2), we consider the following generic discrete first-order dynamics for each dispatched DG asset:

$$\tau^d P_{k+1}^{\mathcal{D},d} = P_k^{\mathcal{D},d} + K_P^d u_k^{P,d} \quad (4a)$$

$$\tau^d Q_{k+1}^{\mathcal{D},d} = Q_k^{\mathcal{D},d} + K_Q^d u_k^{Q,d} \quad (4b)$$

$$(0, -Q_{nom}^{\mathcal{D},d}) \leq (P_k^{\mathcal{D},d}, Q_k^{\mathcal{D},d}) \leq (P_{nom}^{\mathcal{D},d}, Q_{nom}^{\mathcal{D},d}); \quad (4c)$$

$$(-1,-1) \leq (u_k^{P,d}, u_k^{\mathcal{Q},d}) \leq (1,1); \quad (4d)$$

in which (4d) defines the control inputs used to regulate the DG's[3]. (τ^d, K_P^d, K_Q^d) are the DG time constant and nominal DG gains, where the hot-start ramp rates K_P^d/τ^d and K_Q^d/τ^d satisfy $1\% P_{nom}^{\mathcal{D},d}/s$ and $1\% Q_{nom}^{\mathcal{D},d}/s$ [17]. Here we assume that the nominal active/reactive power of the respective DG asset, $(P_{nom}^{\mathcal{D},d}, Q_{nom}^{\mathcal{D},d})$, are determined during sizing and planning phase [18].

C. Optimization metrics for power quality management

The planning and sizing of DG assets, to be dispatched within a microgrid, is often associated with the tertiary control layer. In this instance, it is desirable to determine the placement of DG assets with appropriate sizing within a deterministic network setting which promotes distribution network loss minimization and voltage stability improvements. The sizing (i.e., values for $(P_{nom}^{\mathcal{D},d}, Q_{nom}^{\mathcal{D},d})$ in (4c)) and placement ($d \in \mathcal{D}$) has previously been determined for the Froan case [18]. Here, we consider the voltage profiles and phase angles, $(\bar{V}^i, \bar{\delta}^i)\ \forall i \in \mathcal{M}$ (as evaluated for the ACOPF solution during planning and sizing in [18]) as desirable reference points. To follow are brief formulations to the weighted multiple objectives optimized in the context of dynamic power quality management in aim of promoting increased network resilience.

1) Voltage sag and swell: Voltage sags(or swells) are a reduction(or exceedance) of voltage levels from a desirable nominal voltage level at the bus nodes. These voltage deviations are often considered the most common types of power quality disturbances [19]. In this work we consider managing momentary sags/swells where the IEEE 1159 specification stipulates typical duration's of $0.5-3$s outside the industrial $+/-10\%$ amplitude limit. The weighed objective of interest is:

$$\mathrm{O}_1 := \alpha_1 \|V_k^i - \bar{V}^i\|^2/\bar{V}^i;\ 0 \leq \alpha_1 \leq 1, \forall i \in \mathcal{M} \quad (5)$$

2) Phase angle rate: Over/under frequency- and voltage phase angle-deviations, and Rate of Change of Frequency (RoCoF) are considered effective measures for determining disruptive events, i.e., islanding [20]. In the Froan case, to promote network resiliency, it is desirable to track unwanted voltage phase angle deviations from ideal operation ($\bar{\delta}^i$) whilst minimizing the reliance on grid-tied energy import/export. For the weighted objectives

$$\mathrm{O}_2 := \alpha_2 \|\delta_k^i - \bar{\delta}^i\|^2/\bar{\delta}^i;\ 0 \leq \alpha_2 \leq 1, \forall i \in \mathcal{M} \quad (6a)$$

$$\mathrm{O}_3 := \alpha_3 \left\|P_k^{\mathcal{D},1}\right\|^2 + \alpha_3 \left\|Q_k^{\mathcal{D},1}\right\|^2;\ 0 \leq \alpha_3 \leq 1, \quad (6b)$$

(6a) defines the weighted objective for penalizing voltage phase angle deviations while (6b) implicitly incentivize independence from operating in grid-tied mode.

3) ESS SoC reserves: It has been observed that its advisable to pair ESS assets with solar-PV inverters for networks with high R/X ratios (i.e., rural areas) to achieve satisfactory voltage regulation via reactive power support [21]. To prevent over-, or under-charging of ESS's (in context of uncertain and intermittent RES generation); a desirable metric is to regulate the SoC levels close to $SoC_{ref}^s \approx 50\%$ to ensure sufficient reserves. To such an extent, we consider the weighted objective:

$$\mathrm{O}_4 := \alpha_4 \|SoC_k^{\mathcal{S},s} - SoC_{ref}^{\mathcal{S},s}\|^2/SoC_{ref}^{\mathcal{S},s};\ 0 \leq \alpha_4 \leq 1, \forall s \in \mathcal{S} \quad (7)$$

D. Multi-objective Model Predictive Control formulation

The VVM MPC strategy incorporates the previously defined formulations, introduced in Sections (III-A)-(III-C), into a multi-objective Optimal Control Problem (OCP) which is sequentially solved for each time instant $t, t+h, ..., T$[4]. Here T is some future final time value of operation, and h being the sampling time-rate between successive solutions. For a N-step prediction horizon, at time $t = k$, the VVM MPC is defined as

$$\min_{\mathbf{u}_k(\mathbf{x}_0)} \sum_{k=0}^{N} \left(\sum_{\forall i \in \mathcal{M}} (\mathrm{O}_1 + \mathrm{O}_2) + \mathrm{O}_3 + \sum_{\forall s \in \mathcal{S}} \mathrm{O}_4 \right) \quad (8a)$$

$$s.t.\quad (1), (2), (3), (4) \quad (8b)$$

$$(SoC_k^{\mathcal{S},s}, P_k^{\mathcal{D},d}, Q_k^{\mathcal{D},d}) = (SoC_0^{\mathcal{S},s}, P_0^{\mathcal{D},d}, Q_0^{\mathcal{D},d}) \quad (8c)$$

where $\mathbf{u}_k(\mathbf{x}_0) := [V_k^i, \delta_k^i, u_k^{P,d}, u_k^{Q,d}, P_k^{\mathcal{S}_c,s}, P_k^{\mathcal{S}_d,s}, Q_k^{\mathcal{S},s}]$ defines the generic control vector at time $t = k$ for all $k \in \mathbb{I}_{0:N}$

[3] these can also be associated with potential reference set-points to be communicated to inverters in the primary control layer.

[4] the multi-objectives are summed with tradeoffs stipulated by the respective weights $(\alpha_1, \alpha_2, \alpha_3, \alpha_4)$

given the initial condition $\mathbf{x}_0 := (SoC_0^{\mathcal{S},s}, P_0^{\mathcal{D},d}, Q_0^{\mathcal{D},d})$ (current state of ESS and DG at $t = k$). In the context of MPC, the receding horizon optimal control law is defined as the first stage ($t = k$) of the optimal solution to (8) i.e., $\kappa_N(\mathbf{x}_0) := \mathbf{u}_0^*$. The former control law provides reference set-points for dispatched ESS and DG units within the primary control layer. Observing (measuring) the process states of the dispatched assets one sampling time later (at time $t = k + h$) allows defining new initial conditions which is used to initialize and solve (8) at the next time instant.

E. Computational considerations

MPC has witnessed a widespread adoption in the process industry (associated with slow process dynamics); however, additional numerical challenges need to be overcome to promote numerically feasible and tractable VVM solutions (based on a MPC strategy) which focus on control objectives associated with the secondary and primary control layers for smart microgrid operation. Although not the focus of this work, suggestions will be made in how to obtain faster numerical solutions to (8) as applied for the Froan network. [22] identified three strategies to promote faster numerical solutions for MPC formulations. These are: (i) variable reordering (in terms of control) which reduces MPC complexity from cubic to linear; (ii) warm-start initialization; (iii) enforcing an upper bound on numerical iterations allowing for early sub-optimal termination between successive MPC evaluations. [10] presents a solver which exploits the sparsity of the multi-stage ACOPF problem by means of variable re-ordering. [23] has bench-marked the solution to the ACOPF problem using various linear solvers. It has been concluded, in context of the interior point solver Ipopt, the MA27 and MA57 linear solvers gives superior performance opposed to using the PARDISO solver used in alternative multi-stage ACOPF solver frameworks such as Beltistos.

For this work we solve the VVM MPC problem (8) using Ipopt with MA57 as linear solver and adopt a warm-start strategy. In the warm-start procedure, we initialize subsequent formulations of (8) with optimal primal and dual variables (obtained from optimal solutions to previous optimization evaluations). For the Froan network (including 3 dispatched ESS and DG units), we can solve the related (8) problem with a $N = 15$ prediction horizon on a second scale resolution[5].

IV. Experimental results

As observed by [21], it may be beneficial to dispatch ESS and RES assets at the same bus nodes, due to high R/X ratio's, as is the case for the Froan network. Locations of these assets (busses $[1, 55, 22]$) are chosen in-line with earlier work of [18] which stipulates locations for energy injection based on network loss sensitivities and voltage stability factors. The VVM MPC strategy (8) has a sampling rate of $h = 1$ [s]. Transmission cable failure to the main grid is a rare, but a plausible event, where a resilient system would need

[5]Intel Xeon E-2278G, 3.4-5.0GHz, 32GB

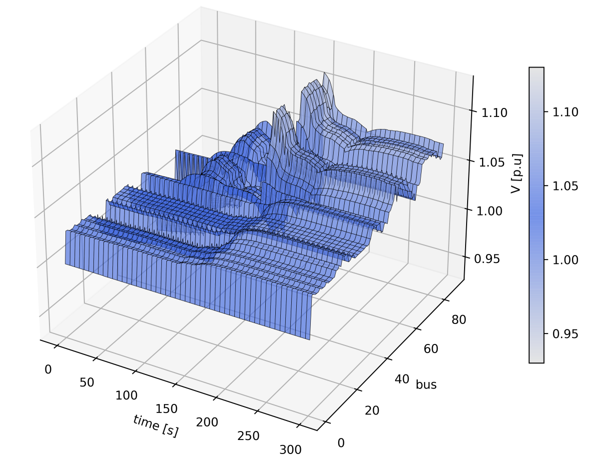

(a) Froan voltage profile [p.u] with disruptive islanding at time $k = 150$ [s] (closed-loop dynamic operation using control law $\kappa_N(\mathbf{x}_0)$ evaluated by solving (8)). Reference bus $i = 1$ satisfy $V = 1$ [p.u].

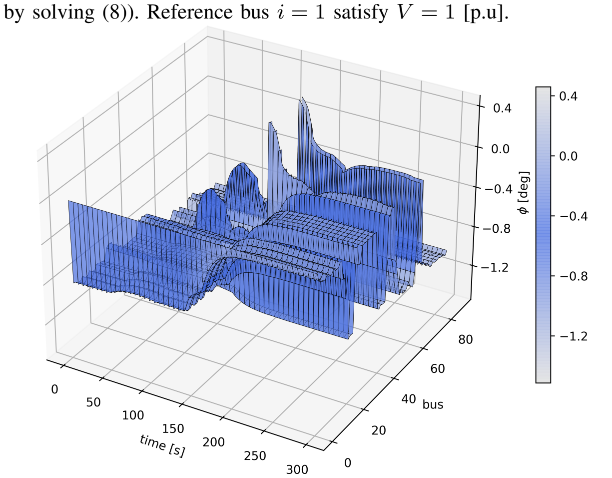

(b) Phase angle closed-loop regulation implementing control law $\kappa_N(\mathbf{x}_0)$. Reference bus $i = 1$ satisfy $\phi = 0$ [deg].

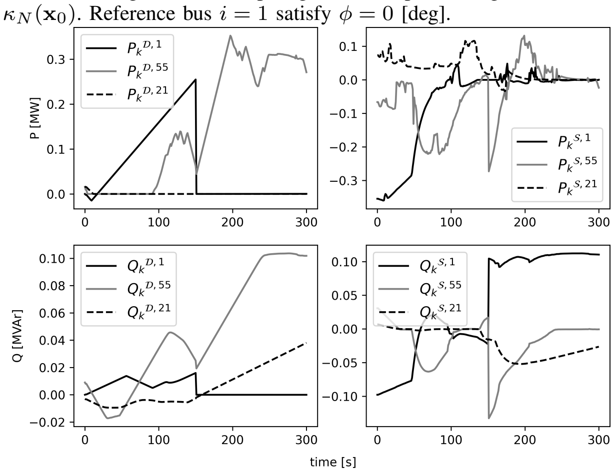

(c) Fast dynamic energy response of dispatched ESS assets to ameliorate effects of islanding whilst accommodating slow ramp-up response of DG assets

Fig. 2: Network resilience for abrupt islanding

to overcome this disturbance. We introduce such an abrupt failure (forcing transition from grid-tied to island mode) at time $t = 150$ [s].

*Note 1 (**Resilient system response**):* Reacting to disruptive faults only on intervals of $h = 1$ [s] may deteriorate the robustness of network resilience. We note, however, on the detection of a fault, one can immediately reevaluate (8), given the new network status, where new control actions can be communicated with the time required to solve (8) (in this work anything from 800 [ms] and upwards depending of network size and assets deployed).

Figures (2a)-(2b) illustrates voltage and phase angle regulation by exploiting network flexibly. Network flexibility exploitation implies using fast responding (intermediate) ESS generation to allow for slow responding DG assets. Figures (2c),(3a) illustrates how ESS assets (when i.e., combined with smart inverters for reactive power support) absorb network faults in the intermediate period before returning back to mid-charged capacity levels. Also part of resilient operation is to absorb the intermittent RES generation as illustrated by Figure (3b).

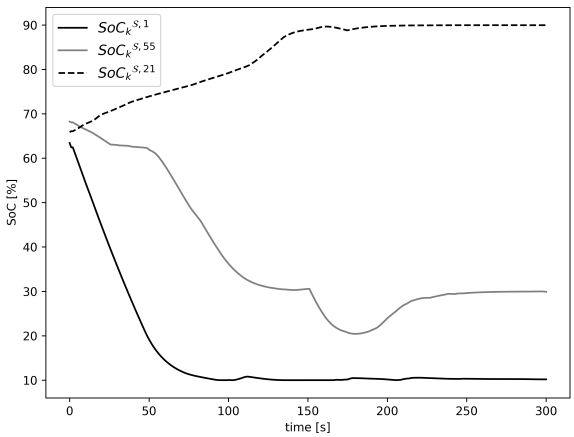

(a) SoC of ESS with fast response dynamics during islanding ($t = 150$ [s]); and, absorption of intermittent RES generation

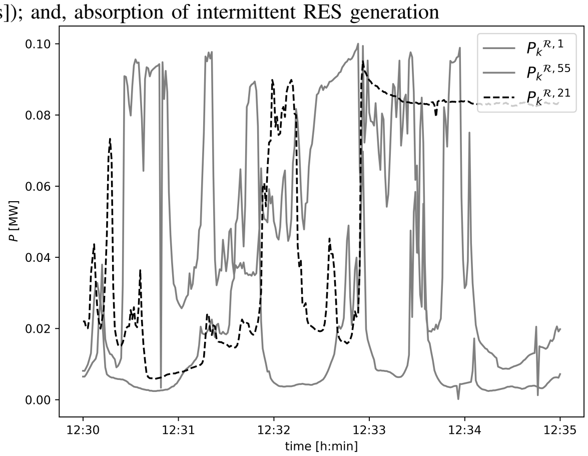

(b) RES (photo-voltaic) power generation for a 5 [min] window of operation

Fig. 3: ESS response in islanding and RES intermittency

V. Concluding remarks

A VVM MPC based strategy has been proposed to promote network resiliency of the Froan network in the event of abrupt transmission line failure. Preliminary results indicate a computationally tractable solution for second-based resolutions. Future work will include agent based, distributed VVM MPC, targeting resilience metrics with sub-second resolutions (ms).

References

[1] D. Gielen, R. Gorini, R. Leme, G. Prakash, N. Wagner, L. Janeiro, S. Collins, M. Kadir, E. Asmelash, R. Ferroukhi, *et al.*, "World energy transitions outlook: 1.5° c pathway," 2021.

[2] S. R. Sinsel, R. L. Riemke, and V. H. Hoffmann, "Challenges and solution technologies for the integration of variable renewable energy sources—a review," *renewable energy*, vol. 145, pp. 2271–2285, 2020.

[3] J. Ma, F. Yang, Z. Li, and S. J. Qin, "A renewable energy integration application in a microgrid based on model predictive control," in *2012 IEEE Power and Energy Society General Meeting*. IEEE, 2012, pp. 1–6.

[4] A. Hussain, V.-H. Bui, and H.-M. Kim, "Microgrids as a resilience resource and strategies used by microgrids for enhancing resilience," *Applied energy*, vol. 240, pp. 56–72, 2019.

[5] K. Rajesh, S. Dash, R. Rajagopal, and R. Sridhar, "A review on control of ac microgrid," *Renewable and sustainable energy reviews*, vol. 71, pp. 814–819, 2017.

[6] J. Hu, Y. Shan, J. M. Guerrero, A. Ioinovici, K. W. Chan, and J. Rodriguez, "Model predictive control of microgrids–an overview," *Renewable and Sustainable Energy Reviews*, vol. 136, p. 110422, 2021.

[7] M. Boloorchi. (2019) Smart grid and power quality management. [Online]. Available: https://smartgrid.ieee.org/newsletters/june-2019/smart-grid-and-power-quality-management

[8] Z. Wang, J. Wang, B. Chen, M. M. Begovic, and Y. He, "Mpc-based voltage/var optimization for distribution circuits with distributed generators and exponential load models," *IEEE Transactions on Smart Grid*, vol. 5, no. 5, pp. 2412–2420, 2014.

[9] P. Li, J. Ji, H. Ji, J. Jian, F. Ding, J. Wu, and C. Wang, "Mpc-based local voltage control strategy of dgs in active distribution networks," *IEEE Transactions on Sustainable Energy*, vol. 11, no. 4, pp. 2911–2921, 2020.

[10] S. Zaferanlouei, H. Farahmand, V. V. Vadlamudi, and M. Korpas, "Battpower toolbox: Memory-efficient and high-performance multi-period ac optimal power flow solver," *IEEE Transactions on Power Systems*, 2021.

[11] J. A. E. Andersson, J. Gillis, G. Horn, J. B. Rawlings, and M. Diehl, "CasADi – A software framework for nonlinear optimization and optimal control," *Mathematical Programming Computation*, vol. 11, no. 1, pp. 1–36, 2019.

[12] A. Wächter and L. T. Biegler, "On the implementation of an interior-point filter line-search algorithm for large-scale nonlinear programming," *Mathematical programming*, vol. 106, no. 1, pp. 25–57, 2006.

[13] P. Cuffe and A. Keane, "Visualizing the electrical structure of power systems," *IEEE Systems Journal*, vol. 11, no. 3, pp. 1810–1821, 2015.

[14] A. Stankovic, "The definition and quantification of resilience," *IEEE PES Industry Technical Support Task Force: Piscataway, NJ, USA*, 2018.

[15] S. Frank and S. Rebennack, "An introduction to optimal power flow: Theory, formulation, and examples," *IIE Transactions*, vol. 48, no. 12, pp. 1172–1197, 2016.

[16] P. Fortenbacher, "On the integration of distributed battery storage in low voltage grids," Ph.D. dissertation, ETH Zurich, 2017.

[17] N. Wägar, "Wind-diesel or wind-gas cases and possibilities by wärtsilä," in *Proc. Int. Wind-Diesel Workshop*, 2008.

[18] S. Das, O. B. Fosso, and G. Marafiot, "A new reliability and security oriented technique for optimal dg placement in a practical distribution network," in *IEEE PowerTech (accepted)*, 2021.

[19] R. P. Bingham, "Sags and swells," *Manager of Technology and Products Dranetz-BMI 1994, Original Draft September 1994 Revised February 16, 1998, New Durham Road Edison, NJ 08818-4019 USA*, 1998.

[20] H. Gabbar, *Smart Energy Grid Engineering*. Academic Press, 2016.

[21] M. N. I. Sarkar, L. G. Meegahapola, and M. Datta, "Reactive power management in renewable rich power grids: A review of grid-codes, renewable generators, support devices, control strategies and optimization algorithms," *IEEE Access*, vol. 6, pp. 41 458–41 489, 2018.

[22] Y. Wang and S. Boyd, "Fast model predictive control using online optimization," *IEEE Transactions on control systems technology*, vol. 18, no. 2, pp. 267–278, 2009.

[23] B. Tasseff, C. Coffrin, A. Wächter, and C. Laird, "Exploring benefits of linear solver parallelism on modern nonlinear optimization applications," *arXiv preprint arXiv:1909.08104*, 2019.